Correlation Functions Calculated by Using Reference Interaction Site Model Equations for Diatomic Molecular Fluids

Kazumitsu Kojima and Kiyoshi Arakawa*

Research Institute of Applied Electricity, Hokkaido University, Sapporo 060

(Received September 25, 1979)

The reference interaction site model (RISM) theory was applied to diatomic molecular fluids, by using three different forms of approximation for site-site direct correlation function. Applicability of the three forms of RISM equation, RISM-1, RISM-2, and RISM-3, was examined, site-site pair correlation functions being calculated from them and a comparison of the results with those of computer simulations being made. Structure factor for liquid nitrogen, oxygen, and bromine were obtained from the solution of the RISM-2 equation and compared with experimental results.

In the preceding paper[1] the authors solved the RISM equation coupled with the Percus-Yevick (PY) and the hypernetted chain (HNC) approximations [referred to as the RISM-1 equation] and applied the result to fluids composed of homonuclear diatomic molecules. Johnson and Hazoumé[2] have also applied the RISM-1 equation coupled with the PY approximation to liquid nitrogen and benzene, and obtained identical results. The original RISM-1 equation was given first intuitively by Chandler and Andersen[3] for molecular fluids composed of fused hard spheres. Chandler[4] derived another form of the equation by means of a systematic functional Taylor expansion [referred to as RISM-2 equation].

The original RISM-1 equation was first solved numerically by Lowden and Chandler[5] for homonuclear diatomic fluids with hard sphere potentials, and used in several numerical works since then. The results were found to be of use for interpreting the behavior of polyatomic fluids.[1,6—9] The result given in the preceding paper[1] shows that the RISM-1 equation can be applied to molecular fluids with an arbitrary site-site pair potential. A graph theoretical interpretation of the RISM-1 equation was given by Chandler.[10]

So far no application of the RISM-2 equation to fluid systems seems to have been carried out. We have undertaken to solve it in combination with a PY and a HNC approximation for fluids composed of homonuclear diatomic molecules in order to compare the results with those obtained from the RISM-1 equation.

The model and three forms of the RISM equation are presented, where a new version of the RISM equation (RISM-3) is proposed in Sec. I, and computational procedures in Sec. II. The results are discussed and compared with those of computer simulations,[11,12] as well as with those of other calculations[13] and experimental studies[14,15] in Sec. III. The HNC approximation for RISM-2 equation are given in Appendix by means of the functional Taylor expansion.

Theory

Model and Definition of Statistical Mechanical Functions.[1]
Let us consider the same system as that treated previously.[1] The molecular shape is shown in Fig. 1. An intermolecular potential, $w(i,j)$, is expressed as the sum of site-site pair interaction potentials $u_{\alpha\gamma}(|\mathbf{r}_i^\alpha - \mathbf{r}_j^\gamma|)$.
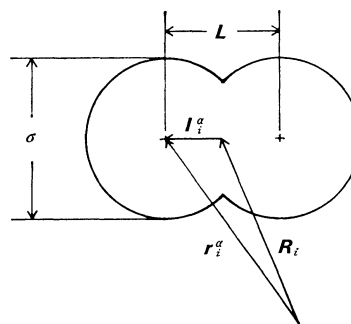

Fig. 1. Shape of RISM molecule.

Two types of site-site pair potentials were chosen: the Lennard-Jones potential[1] and the hard sphere potential,

$$u_{\alpha\gamma}(r) = \infty, \quad r < \sigma, \quad \Big\}$$
$$= 0, \quad r > \sigma, \quad \Big\} \tag{1}$$

where σ is the diameter of the hard sphere.

The site-site total correlation function, $h_{\alpha\gamma}(r) = g_{\alpha\gamma}(r) - 1$, is considered, the site-site pair correlation function, $g_{\alpha\gamma}(r)$, being defined as reported.[1] The site-site direct correlation function, $c_{\alpha\gamma}(r)$, is defined by an Ornstein-Zernike type equation[4,10] as

$$\mathbf{h}(r) = \boldsymbol{\omega}*\mathbf{c}*\boldsymbol{\omega}(r) + \rho\boldsymbol{\omega}*\mathbf{c}*\mathbf{h}(r) \tag{2}$$

where the * denotes a convolution, ρ the number density and the matrices $\mathbf{h}(r)$, $\boldsymbol{\omega}(r)$, and $\mathbf{c}(r)$ have element $h_{\alpha\gamma}(r)$, $\omega_{\alpha\gamma}(r)$, and $c_{\alpha\gamma}(r)$, respectively. The first term of $h_{\alpha\gamma}(r)$ in Eq. 2 is expressed as

$$\sum_{\eta,\nu} \int d\mathbf{r}' \int d\mathbf{r}'' \omega_{\alpha\eta}(\mathbf{r}'')c_{\eta\nu}(|\mathbf{r}''-\mathbf{r}'|)\omega_{\nu\gamma}(|\mathbf{r}'-\mathbf{r}|). \tag{3}$$

The function, $\omega_{\alpha\gamma}(r)$, for the rigid diatomic molecule is expressed as

$$\omega_{\alpha\gamma}(r) = \delta_{\alpha\gamma}\delta(r) + (1-\delta_{\alpha\gamma})(4\pi L_{\alpha\gamma}^2)^{-1}\delta(r-L_{\alpha\gamma}),^{18)} \tag{4}$$

where, $\delta(r)$ and $\delta_{\alpha\gamma}$ are the Dirac delta function and the Kronecker delta, respectively. The Fourier transform representation of Eq. 2 is

$$\hat{\mathbf{h}}(\mathbf{k}) = \hat{\boldsymbol{\omega}}(\mathbf{k})\hat{\mathbf{c}}(\mathbf{k})\hat{\boldsymbol{\omega}}(\mathbf{k})[\mathbf{1} - \rho\hat{\mathbf{c}}(\mathbf{k})\hat{\boldsymbol{\omega}}(\mathbf{k})]^{-1}, \tag{5}$$

where $\mathbf{A}^{-1}$ denotes the matrix inverse of a matrix $\mathbf{A}$ and $\mathbf{1}$ the identity matrix.

PY and HNC Approximations. The PY and HNC approximations for the RISM-1 equations[1] are expressed as

$$c_{\alpha\gamma}(r) = y_{\alpha\gamma}'(r)f_{\alpha\gamma}(r) \tag{6}$$

and

$$c_{\alpha\gamma}(r) = y'_{\alpha\gamma}(r)[f_{\alpha\gamma}(r)+1] - \ln y'_{\alpha\gamma}(r) - 1, \qquad (7)$$

respectively. Here the $f_{\alpha\gamma}(r)$ and the $y'_{\alpha\gamma}(r)$ are defined by

$$f_{\alpha\gamma}(r) = \exp[-\beta u_{\alpha\gamma}(r)] - 1, \qquad (8)$$

and

$$y'_{\alpha\gamma}(r) = g_{\alpha\gamma}(r)[f_{\alpha\gamma}(r)+1]^{-1}, \qquad (9)$$

respectively, where the β^{-1} is equal to the Boltzmann constant multiplied by temperature.

Chandler[4] derived the PY approximation for the RISM-2 equation by means of a systematic functional Taylor expansion. The functional form of the PY approximation for the RISM-2 equation is

$$[\omega*c*\omega(r)]_{\alpha\gamma} = y_{\alpha\gamma}(r)\bar{f}_{\alpha\gamma}(r), \qquad (10)$$

where the $y_{\alpha\gamma}(r)$ and the $\bar{f}_{\alpha\gamma}(r)$ are defined by

$$y_{\alpha\gamma}(r) = g_{\alpha\gamma}(r)[\bar{f}_{\alpha\gamma}(r)+1]^{-1}, \qquad (11)$$

and

$$\bar{f}_{\alpha\gamma}(r) = \int d\mathbf{1} d2\delta(\mathbf{r}^{\alpha})\delta(\mathbf{r}^{\gamma}-\mathbf{r})\{\prod_{\eta,\nu}[f_{\eta\nu}(r)+1]-1\}, \qquad (12)$$

respectively. The $\bar{f}_{\alpha\gamma}(r)$ is the averaged Mayer function when site α on molecule 1 and site γ on molecule 2 are held fixed at a distance r from each other. Let us propose the HNC approximation for the RISM-2 equation expressed as

$$[\omega*c*\omega(r)]_{\alpha\gamma} = y_{\alpha\gamma}(r)[\bar{f}_{\alpha\gamma}(r)+1] - \ln y_{\alpha\gamma}(r) - 1. \qquad (13)$$

The equation is derived by means of the functional Taylor expansion (see Appendix).

Further, let us propose new approximations (RISM-3) in analogy with Eqs. 6, 10 (PY), and Eqs. 7, 13 (HNC) as follows:

$$[\omega*c*\omega(r)]_{\alpha\gamma} = y'_{\alpha\gamma}(r)f_{\alpha\gamma}(r), \qquad (14)$$

and

$$[\omega*c*\omega(r)]_{\alpha\gamma} = y'_{\alpha\gamma}(r)[f_{\alpha\gamma}(r)+1] - \ln y'_{\alpha\gamma}(r) - 1, \qquad (15)$$

respectively. Equations 14 and 15 are similar to the PY and HNC approximations in their functional form, respectively.

Three Forms of the RISM Equation. Various forms of integral equations are given by combining Eq. 5 (Ornstein-Zernike type equation) with one of several types of the PY and HNC approximations. We call Eq. 5 coupled with Eq. 14 or Eq. 15 the RISM-3 equation. The RISM-1 equation[1] is expressed as Eq.5 coupled with Eq. 6 or Eq. 7. The RISM-2 equation[4] is expressed as Eq. 5 coupled with Eq. 10 or Eq. 13. The RISM-1 equation was solved[1] in the case of fluids composed of homonuclear diatomic molecules (Fig. 1), interacting through the Lennard-Jones site-site pair potential. Solutions of the RISM-2 and 3 equation have been obtained for the first time in the case of homonuclear diatomic fluids.

Computational Procedure

Computational Methods. The procedure to solve the RISM-1 equation was reported.[1] The RISM-2 equation was solved by means of an iteration procedure. The functions $h_{\alpha\gamma}(r)$ and $[\omega*c*\omega(r)]_{\alpha\gamma}$ have a dis-

continuity at $r=\sigma_{\alpha\gamma}$. Thus, we define a new function $\gamma_{\alpha\gamma}(r)$,

$$\gamma_{\alpha\gamma}(r) \equiv h_{\alpha\gamma}(r) - C_{\alpha\gamma}(r), \qquad (16)$$

where

$$C_{\alpha\gamma}(r) \equiv [\omega*c*\omega(r)]_{\alpha\gamma}. \qquad (17)$$

$\gamma_{\alpha\gamma}(r)$ is a continuous function of r. By use of it, the RISM-2 equation can be written as

$$\hat{\gamma}(k) = \hat{C}(k)\hat{\omega}^{-1}(k)\hat{C}(k)[1 - \rho\hat{\omega}^{-1}(k)\hat{C}(k)]^{-1}, \qquad (18)$$

and

$$\gamma_{\alpha\gamma}(r) = y_{\alpha\gamma}(r) - 1 \qquad (PY),$$
$$= \ln y_{\alpha\gamma}(r) \qquad (HNC). \qquad (19)$$

The initial choise for $y_{\alpha\gamma}(r)$ is $y_{\alpha\gamma}(r)=1$, because the $h_{\alpha\gamma}(r)$ is equal to $\bar{f}_{\alpha\gamma}(r)$ at the low density limit. The iteration has been continued until the self-consistency of

$$\left|\frac{y_{\alpha\gamma}^{out}(r) - y_{\alpha\gamma}^{in}(r)}{y_{\alpha\gamma}^{in}(r)}\right| < 10^{-7} \qquad (20)$$

is satisfied.

Calculation of the Function $\bar{f}_{\alpha\gamma}(r)$. For the diatomic molecule, the $\bar{f}_{\alpha\gamma}(r_1^{\alpha}, r_2^{\gamma})$ is represented by Ladanyi and Chandler[16] as follows.

$$\bar{f}_{\alpha\gamma}(r_1^{\alpha}, r_2^{\gamma}) = \text{[diagrammatic expression]} \qquad (21)$$

where $\circ\!\!-\!\!\circ$ and $\circ\!\!\sim\!\!\circ$ represent $f_{\alpha\gamma}(r_1^{\alpha}, r_2^{\gamma})$ and $s_{\alpha\gamma}(r_1^{\alpha}, r_2^{\gamma})$, respectively. White circles are labeled since they represent particular interaction site at specific locations. Black circles are circles which have been integrated over space and summed over interaction site, *i.e.*

$$\bullet = \sum_{\alpha=1}^{m} \int d\mathbf{r}_1^{\alpha}[O_1].$$

For example, the diagram [diagram] represents the integral $\sum_{\eta=1}^{m} \int d\mathbf{r}^{\eta} f_{\alpha\eta}(r_1^{\alpha}, r^{\eta}) s_{\eta\gamma}(r^{\eta}, r_2^{\gamma})$. The last two diagrams of Eq. 21 are omitted because the contribution of these two terms is negligible in the case of hard sphere site-site pair potential.[16]

Calculation of Structure Factors. Neutron scattering experiments can determine the structure factor, $S(k)$, which is expressed in terms of site-site pair correlation functions:

$$S(k) = (\sum_{\alpha=1}^{m} b_\alpha)^{-2} \sum_{\alpha,\gamma}^{m} b_\alpha b_\gamma[\hat{\omega}_{\alpha\gamma}(k) + \rho\hat{h}_{\alpha\gamma}(k)], \qquad (22)$$

where the b_α denotes the coherent neutron scattering amplitude for a nucleus of type α. We carried out the calculations of the structure factors for liquid nitrogen, oxygen and bromine. In order to compare the results with those obtained from experimental studies,[14,15] it is neccesary to determine two molecular

TABLE 1.

	σ/nm	L/nm	L/σ
N_2	0.33	0.11	0.3
O_2	0.295	0.12	0.407
Br_2	0.33	0.228	0.691

parameters, σ and L, of these diatomic molecules. Hsu et al.[9] used the best parameters of the molecules by a comparison of the structure factors calculated with those obtained by experiments.[14,15] The molecular parameters in the present calculations are given in Table 1.

Results and Discussion

Correlation Functions. Figure 2 shows the function, $g_{11}(r)$, calculated by means of the RISM-1, 2, and 3 equations by the use of the PY approximation for diatomic fluids with the hard sphere site-site pair potentials. The $g_{11}(r)$ calculated from the RISM-3 equation is similar in shape to a $g(r)$ of simple hard-sphere fluids. The $g_{11}(r)$ calculated from the RISM-2 equation is in good agreement with that calculated by means of the RISM-1 equation except in the vicinity of first peak. It seems that the difference in the vicinity of the two first peaks results from the use of the two different forms of PY approximations, Eqs. 6 and 10. Figure 3 shows the function $g_{11}(r)$ calculated by the RISM-1, 2, and 3 equations for fluids with the Lennard-Jones site-site pair potentials by the use of the PY approximations as well as the curve obtained by molecular dynamics study.[11] The function $g_{11}(r)$ calculated from the RISM-1 equation is in best agreement with the result of molecular dynamics. It is evident from Fig. 2 that two $g_{11}(r)$ curves calculated by the use of the RISM-1 and 2 equations for hard-sphere fluids are nearly identical with each other over the region $r \geq \sigma + L$, in sharp contrast to the cases of the Lennard-Jones fluids (Fig. 3).

Figure 4 shows $g_{11}(r)$ calculated by the RISM-2 equation with use of the PY approximation for the fluid with the hard sphere site-site pair potential at two densities. $g_{11}(r)$ at $\rho\sigma^3 = 0.4$ has a sharp cusp at $r = \sigma + L$, while at a higher density, $\rho\sigma^3 = 0.65$, a weak square shoulder appears at the same position. At a higher density, the shape of the first peak of the RISM-2 equation differs to some extent from that of the RISM-1 equation as seen by a comparison of Figs. 2 and 4. Figure 5 shows $g_{11}(r)$ calculated by the RISM-2 equation with use of the PY approximation for fluids with the Lennard-Jones site-site pair potentials at two densities, $\rho\sigma^3 = 0.4$ and 0.65, and at the same temperature, $kT/\varepsilon = 4.03$.

Johnson[13] derived a new equation analogous to the RISM-1 equation from the Ornstein-Zernike equation using Fourier-Wigner series, and calculated $g_{11}(r)$ for fluids with hard-sphere site-site potentials. Figure 6 shows a comparison of $g_{11}(r)$ we obtained with Johnson's. Our $g_{11}(r)$ has a shoulder at $r = \sigma + L$ in contrast to the results obtained by Johnson.
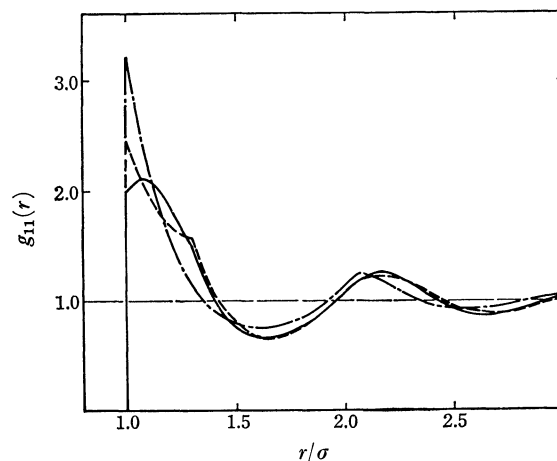
Figure 7 shows $g_{11}(r)$ calculated by the RISM-2

Fig. 2. Site-site pair correlation functions calculated by using the PY like approximation for diaomic molecular fluids with the hard sphere potential: $L/\sigma = 0.3$ and $\rho\sigma^3 = 0.6964$.
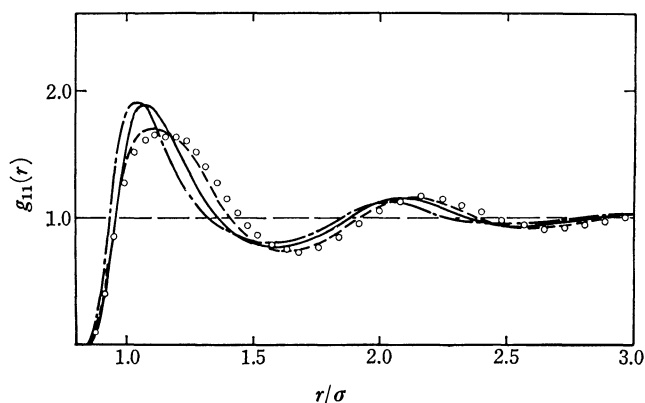----: RISM-1, ——: RISM-2, ——–: RISM-3.

Fig. 3. Site-site pair correlation functions calculated by using the PY like approximation for diatomic molecular fluids with the Lennard-Jones potential: $L/\sigma = 0.3$, $\rho\sigma^3 = 0.6964$ and $kT/\varepsilon = 4.03$.
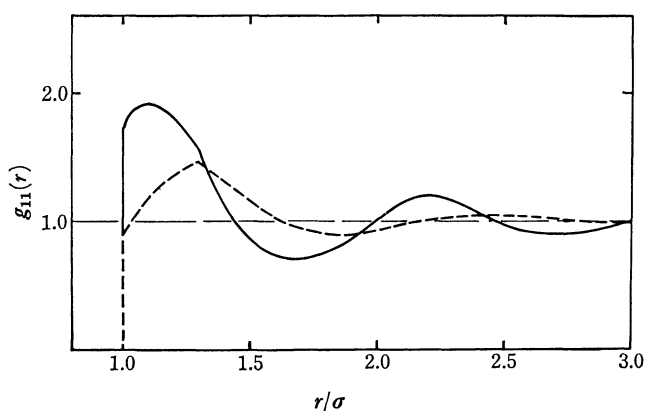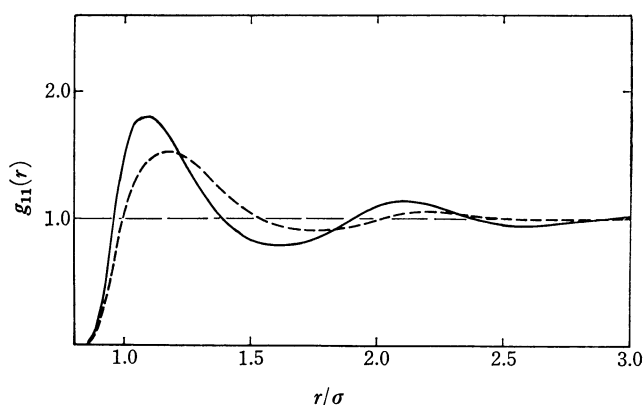----: RISM-1, ——: RISM-2, ——–: RISM-3, oooo: molecular dynamics result of Ref. 11.

Fig. 4. Site-site pair correlation functions calculated from the RISM-2 equation by using the PY like approximation for diatomic molecular fluids with the hard-sphere potential: $L/\sigma = 0.3$.
----: $\rho\sigma^3 = 0.4$, ——: $\rho\sigma^3 = 0.65$.

Fig. 5. Site-site pair correlation functions calculated from the RISM-2 equation by using the PY like approximation for diatomic molecular fluids with the Lennard-Jones potential: $L/\sigma = 0.3$ and $kT/\varepsilon = 4.03$. ----: $\rho\sigma^3 = 0.4$, ——: $\rho\sigma^3 = 0.65$.
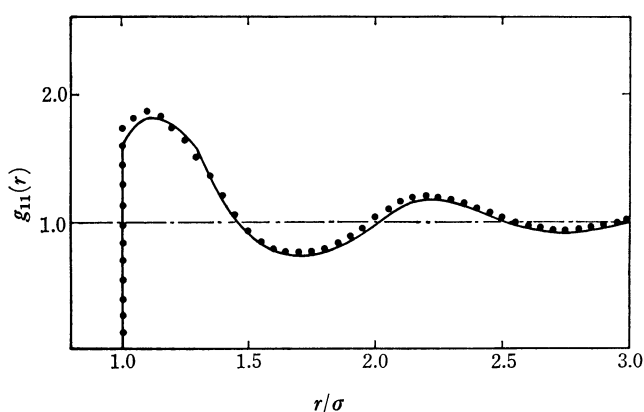

Fig. 6. Site-site pair correlation functions for diatomic molecular fluids with the hard sphere potential: $L/\sigma = 0.3$ and $\rho\sigma^3 = 0.6214$.
——: This work (RISM-2, PY like approximation),
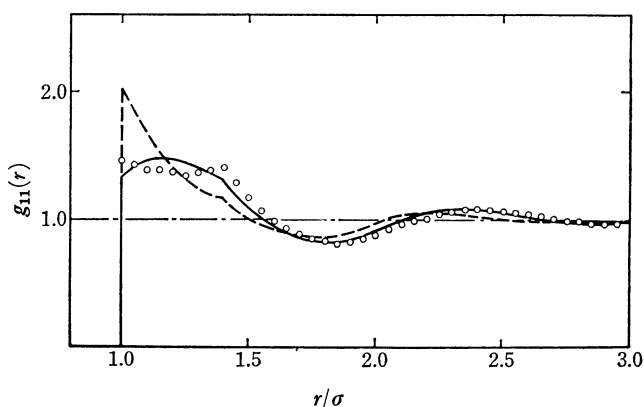••••: calculated result of Ref. 13.

Fig. 7. Site-site pair correlation functions calculated from the RISM-2 equation for diatomic molecular fluids with the hard-sphere potential: $L/\sigma = 0.4$ and $\rho\sigma_3 = 0.4875$.
——: PY like approximation, ----: HNC like approximation, ○○○○: Monte Carlo result of Ref. 12.

equation with use of the PY approximation as well as that obtained by the Monte Carlo (MC) method.[12] $g_{11}(r)$ calculated with use of the PY approximation is in better agreement with the result of MC calculation as compared with that calculated with use of the HNC approximation. Figure 8 shows a comparison of the site-site direct correlation function, $c_{11}(r)$, with results calculated with use of the PY and HNC approximations, including those of MC calculation. $c_{11}(r)$ calculated with use of the PY approximation is in agreement with that obtained by the MC calculation within the range from the origin to $r = \sigma - L$.

Structure Factors. Structure factors calculated with use of the RISM-2 equation are compared with those determined by neutron scattering experiments (Figs. 9—11). Calculations were carried out with use of the RISM-2 equation with the PY approximation
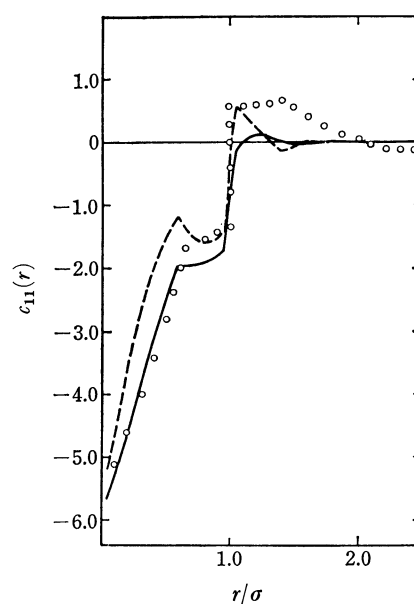

Fig. 8. Site-site direct correlation functions, $c_{11}(r)$, calculated from the RISM-2 equation for diatomic molecular fluids with the hard-sphere potential: $L/\sigma = 0.3$ and $\rho\sigma^3 = 0.4875$.
——: PY like approximation, ----: HNC like approximation, ○○○○: Monte Carlo result of Ref. 12.
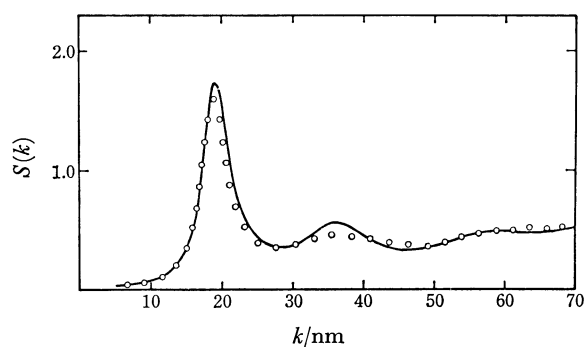

Fig. 9. Comparison of structure factors between calculated and experimental results for liquid nitrogen.
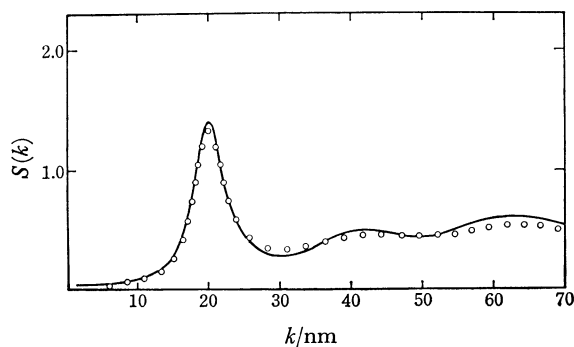——: This work, ○○○○: experimental result of Ref. 14.

Fig. 10. Comparison of structure factors between calculated and experimental results for liquid oxygen. ———: This work, ○○○○: experimental result of Ref. 14.
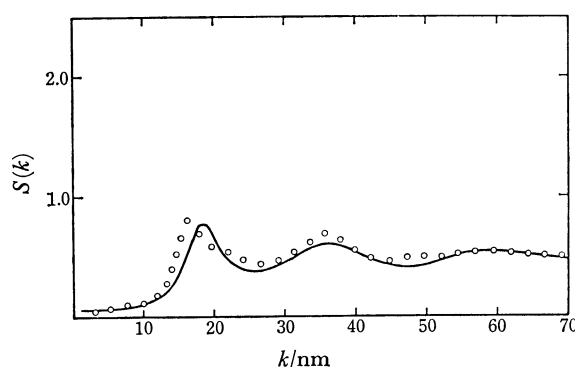

Fig. 11. Comparison of structure factors between calculated and experimental results for liquid bromine. ———: This work, ○○○○: experimental result of Ref. 15.

for diatomic molecular fluids with hard sphere site-site pair potentials. The experimental results are those for liquid nitrogen,[14] oxygen,[14] and bromine[15] under the conditions given in Table 2. The molecular parameters for these liquids[12] are given in Table 1.

The agreement between calculated and experimental results is satisfactory in the cases of liquid nitrogen and liquid oxygen. In liquid bromine, the calculated values deviate from the experimental ones in the vicinity of the first and second peaks. Experimental studies[15] show that the behavior of $S(k)$ of liquid bromine is in sharp contrast to that of liquid nitrogen and liquid oxygen.

The $S(k)$ curves calculated by the RISM-1 and the RISM-2 equations are in good agreement with those obtained from experiment,[1,6,9] for liquid nitrogen and liquid oxygen. The discrepancy between calculated and experimental results for liquid bromine seems to be ascribed to some characteristic of the liquid.[17]

Comparison of the Three Forms of the RISM Equation.

Summarizing the results in the present and preceding paper,[1] we can say that the RISM-1 equation gives the best results, viz., the presence of a cusp or a shoulder at $r=\sigma+L$ in $g_{\alpha r}(r)$ curves and agreement of the curves with those given by MD calculations. The numerical results of $g_{\alpha r}(r)$ show that the RISM-1 equation is the best of the three equations, the RISM-2

coming next. Concerning the structure factor curves, the RISM-2 equation seems to give as good results as the RISM-1 equation (Fig. 9 and 10, and Ref. 1).

Of the three equations the RISM-1 equation behaves the best on the whole, but it contains some "unallowed diagrams" as stated by Chandler from the viewpoint of topological reduction scheme.[10] In a strict sence the RISM-1 equation contains inconsistensy in its theoretical scheme Thus the RISM-2 equation derived by systematic functional Taylor expansion[4] might be superior to the RISM-1 equation, though the latter is fairly easy to treat in calculation as compared with the other two equations.

Appendix

The HNC approximation for the RISM-2 equation is derived as follows by means of the method of a generalized functional Taylor expansion proposed by Chandler.[4]

Consider the quantity

$$Q_{\alpha r}(r, \phi) = \langle \rho_r(r) \rangle_\phi \Big[\int d\mathbf{1} d\mathbf{2} \delta(r_1^\alpha) \delta(r_2^r - r)$$

$$\times \exp\{-\beta \sum_{\eta, \nu} \phi_{\eta \nu}(r_2^\nu - r_1^\eta)\} \Big]^{-1}, \qquad (A-1)$$

where the function $\phi_{\eta \nu}(r_2 - r_1)$ denotes an arbitrary site-site potential function.

At the end points

$$\int d\mathbf{1} \delta(r_1^\alpha) Q_{\alpha r}(r, \phi=0) = \rho \qquad (A-2)$$

and

$$\int d\mathbf{1} \delta(r_1^\alpha) Q_{\alpha r}(r, \phi=u) = \rho g_{\alpha r}(r) [\overline{f}_{\alpha r}(r) + 1]^{-1}. \qquad (A-3)$$

We define a new quantity, $Q'_{\alpha r}(r, \phi)$, by

$$Q'_{\alpha r}(r, \phi) \equiv \ln \Big[\int d\mathbf{1} \delta(r_1^\alpha) Q_{\alpha r}(r, \phi) \Big]. \qquad (A-4)$$

If we expand $Q'_{\alpha r}(r, \phi)$ in powers of the response

$\langle \rho_\eta(r') \rangle_u - \rho$:

$$Q'_{\alpha r}(r, u) = Q'_{\alpha r}(r, 0)$$

$$+ \sum_\eta \int dr' \frac{\delta Q'_{\alpha r}(r, \phi)}{\delta \langle \rho_\eta(r') \rangle_\phi} \Big|_{\phi=0} [\langle \rho_\eta(r') \rangle_u - \rho]$$

$$+ \cdots \qquad (A-5)$$

Truncating the right hand side of Eq. (A-5) at linear term, we can calculate the term by the use of the relations Eqs. (3.4) and (3.5) in Ref. 4, and obtain

$$\sum_\eta \int dr' \frac{\delta Q'_{\alpha r}(r, \phi)}{\delta \langle \rho_\eta(r') \rangle_\phi} \Big|_{\phi=0} [\langle \rho_\eta(r') \rangle_u - \rho] =$$

$$h_{\alpha r}(r) - [\omega * c * \omega(r)]_{\alpha r}.$$

Substituing Eqs. A-2, A-3, and A-6 into Eq. A-5, we get

$$[\omega * c * \omega(r)]_{\alpha r} = h_{\alpha r}(r) - \ln g_{\alpha r}(r) [\overline{f}_{\alpha r}(r) + 1]^{-1}.$$

The relation is the HNC approximation for RISM-2 equation.

TABLE 2.

	ρ/nm^{-3}	T/K
N_2	17.29	77.4
O_2	21.98	84
Br_2	11.76	293

References

1) K. Kojima and K. Arakawa, *Bull. Chem. Soc. Jpn.*, **51**, 1977 (1978).

2) E. Johnson and R. P. Hazoumé, *J. Chem. Phys.*, **70**, 1599 (1979).

3) D. Chandler and H. C. Andersen, *J. Chem. Phys.*, **57**, 1930 (1972).

4) D. Chandler, *J. Chem. Phys.*, **59**, 2742 (1973).

5) L. J. Lowden and D. Chandler, *J. Chem. Phys.*, **59**, 6587 (1973).

6) L. J. Lowden and D. Chandler, *J. Chem. Phys.*, **61**, 5228 (1974).

7) B. C. Freasier, D. Jolly, and R. J. Bearman, *Mol. Phys.*, **32**, 1463 (1976).

8) C. S. Hsu and D. Chandler, *Mol. Phys.*, **36**, 215 (1978).

9) C. S. Hsu, D. Chandler, and L. J. Lowden, *Chem. Phys.*, **14**, 213 (1976).

10) D. Chandler, *Mol. Phys.*, **31**, 1213 (1976).

11) J. Barojas, D. Levesque, and B. Quentrec, *Phys. Rev. A*, **7**, 1902 (1972); B. Quentrec and C. Brot, *ibid.*, **12**, 272 (1975).

12) W. B. Streett and D. J. Tildesley, *J. Chem. Phys.*, **68**, 1275 (1978).

13) E. Johnson, *J. Chem. Phys.*, **67**, 3194 (1977).

14) J. C. Dore, G. Walford, and D. I. Page, *Mol. Phys.*, **29**, 565 (1975).

15) J. H. Clarke, J. C. Dore, G. Walford, and R. N. Sinclair, *Mol. Phys.*, **31**, 883 (1976); G. W. Stanton, J. H. Clarke, and J. C. Dore, *ibid.*, **34**, 823 (1977).

16) B. M. Ladanyi and D. Chandler, *J. Chem. Phys.*, **62**, 4309 (1975).

17) Clarke *et al.* state that "the difference may be attributed to the increased anisotropy and vibrational properties of bromine molecules."[15]

18) We correct the careless mistake of dropping the power index 2 of $L_{\alpha\gamma}$ in Eq. 6 of the preceding paper.[1]